

Excitation of accelerating plasma waves by counter-propagating laser beams^{a)}

Gennady Shvets^{b)} and Nathaniel J. Fisch
Princeton Plasma Physics Laboratory, Princeton, New Jersey 08543

Alexander Pukhov
Max-Planck-Institut für Quantenoptik, D-85748 Garching, Germany

(Received 2 November 2001; accepted 19 February 2002)

The conventional approach to exciting high phase velocity waves in plasmas is to employ a laser pulse moving in the direction of the desired particle acceleration. Photon downshifting then causes momentum transfer to the plasma and wave excitation. Novel approaches to plasma wake excitation, colliding-beam accelerator (CBA), which involve photon exchange between the long and short counter-propagating laser beams, are described. Depending on the frequency detuning $\Delta\omega$ between beams and duration τ_L of the short pulse, there are two approaches to CBA. First approach assumes ($\tau_L \approx 2/\omega_p$). Photons exchanged between the beams deposit their recoil momentum in the plasma driving the plasma wake. Frequency detuning between the beams determines the direction of the photon exchange, thereby controlling the phase of the plasma wake. This phase control can be used for reversing the slippage of the accelerated particles with respect to the wake. A variation on the same theme, super-beatwave accelerator, is also described. In the second approach, a short pulse with $\tau_L \gg \omega_p^{-1}$ detuned by $\Delta\omega \sim 2\omega_p$ from the counter-propagating beam is employed. While parametric excitation of plasma waves by the electromagnetic beatwave at $2\omega_p$ of two *co-propagating* lasers was first predicted by Rosenbluth and Liu [M. N. Rosenbluth and C. S. Liu, Phys. Rev. Lett. **29**, 701 (1972)], it is demonstrated that the two excitation beams can be *counter-propagating*. The advantages of using this geometry (higher instability growth rate, insensitivity to plasma inhomogeneity) are explained, and supporting numerical simulations presented. © 2002 American Institute of Physics. [DOI: 10.1063/1.1468649]

I. INTRODUCTION AND MOTIVATION

Plasma is an attractive medium for ultrahigh gradient particle acceleration because it can sustain a very high electric field, roughly limited by the cold wavebreaking field $E_{WB} = mc\omega_p/e \approx \sqrt{n}[\text{cm}^{-3}]\text{V/cm}$, where $\omega_p = \sqrt{4\pi e^2 n/m}$ is the plasma frequency and n is the electron density. To accelerate injected particles to velocities close to the speed of light c , this electric field has to be in a form of a fast longitudinal plasma wave with phase velocity $v_{ph} \approx c$. The frequency of the fast plasma wave is ω_p , and its wave number is $k_p \approx \omega_p/c$. Excitation of such plasma waves can be accomplished by lasers or fast particle beams.¹⁻¹³

Below we review the basics of linear plasma wave excitation in very general terms, without restricting ourselves to the specifics of the wakefield driver. Let us assume that plasma electrons are subject to the electric field of the fast plasma wave \mathbf{E} , as well as other nonlinear forces \mathbf{F}_{NL} , for example, the ponderomotive force of one or more laser pulses. The total current $\mathbf{J} = \mathbf{J}_p + \mathbf{J}_2$ which enters Ampère's law $\nabla \times \mathbf{B} = (1/c)\partial_t \mathbf{E} + (4\pi/c)(\mathbf{J}_p + \mathbf{J}_2)$ is intentionally split into two components. The first one, $\mathbf{J}_p = -en\mathbf{v}_e$, where \mathbf{v}_e is the electron fluid velocity, is driven by the electric field \mathbf{E} and satisfies $\partial_t \mathbf{J}_p = e^2 n \mathbf{E}$. The second component \mathbf{J}_2 is

driven by the nonlinear ponderomotive force, or could also represent an external current provided by injected electron beam. Taking the time derivative of the Ampère's law yields:

$$\left(\frac{\partial^2}{\partial t^2} + \omega_{p0}^2\right)\mathbf{E} + c^2 \nabla \times \nabla \times \mathbf{E} = -4\pi \frac{\partial \mathbf{J}_2}{\partial t}, \quad (1)$$

where the $\nabla \times \nabla \times \mathbf{E}$ term naturally vanishes in one-dimensional (1D). One can say that the science of making a plasma accelerator is about finding the most effective way of producing the appropriate $J_{2z}(z, t)$. Of course, not every functional form of $J_{2z}(z, t)$ is useful for making plasma waves suitable for relativistic particle acceleration. In the rest of this paper we concentrate on exciting $J_{2z}(z, t) \equiv J_{2z}(z - ct)$ using one or several laser pulses.

II. COMPARISON OF SINGLE-BEAM AND COLLIDING BEAM ACCELERATORS

The simplest laser-driven plasma accelerator, which was also the first one realized in the experiments, is the plasma beatwave accelerator¹⁻⁶ (PBWA). It employs a pair of co-propagating laser beams with normalized vector-potentials $\mathbf{a}_{0,1} = e\mathbf{A}_{0,1}/mc^2$ and frequencies ω_0 and $\omega_1 = \omega_0 - \omega_p$. The nonlinear current J_{2z} is driven by the ponderomotive force of the resulting electromagnetic beatwave according to $\partial_t J_{2z} = en\partial_z(\mathbf{a}_0 \cdot \mathbf{a}_1)$. If the two laser-beams are detuned by the

^{a)}Paper G12 3, Bull. Am. Phys. Soc. **46**, 136 (2001).

^{b)}Invited speaker.

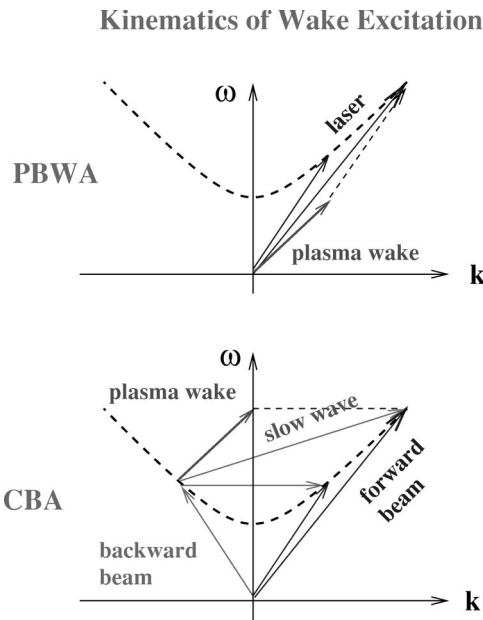


FIG. 1. PBWA: Kinematics of the plasma wake excitation by a co-propagating wave packet consisting of two frequency components differing by $\Delta\omega = \omega_p$. Phase velocity of plasma wake $v_{ph} \approx v_g$, where v_g is the group velocity of the wave packet; CBA: Same, only using an extra counter-propagating laser beam. Nonlinear beating of two slow waves gives rise to fast plasma wake.

plasma frequency ω_p , plasma wave is resonantly excited. The beatwave scheme was also considered by Rosenbluth and Liu¹⁴ for plasma heating.

From Eq. (1), to excite a plasma wave one needs to deposit momentum into the plasma. The source of this momentum is the laser. However, since the typical laser frequencies $\omega_{0,1} \gg \omega_p$, it is impossible for a laser photon to impart its entire momentum to the plasma. What happens instead is that the frequency of a laser photon is down-shifted by the amount ω_p , depositing the remainder momentum and energy into the plasma. In the case of PBWA, higher-frequency photons at ω_0 are scattered into the lower-frequency photons at $\omega_1 = \omega_0 - \omega_p$. Schematically, this process is shown in the top Fig. 1. The phasors of the lasers lie on the $\omega^2 = \omega_p^2 + c^2 k^2$ dispersion curve, and the vector difference of these phasors gives the phasor of the driven plasma wave. Phase velocity of the plasma wave is then given by $v_{ph} = (\omega_0 - \omega_1) / (k_0 - k_1) \approx v_g$, where $v_g \approx c(1 - \omega_p^2 / 2\omega_0^2)$ is the group velocity of the laser packet. Since $v_{ph} \approx c$, thus excited plasma wave is suitable for particle acceleration.

The total momentum transfer rate to the plasma in PBWA is then proportional to the relative momentum transfer per photon $\eta_t = \omega_p / \omega_0$, times the rate of scattering which is proportional to beam intensity. Since the relative amount of down-shifting $\eta_t \ll 1$, high laser intensities are needed to ensure the high overall rate of the momentum transfer. Note that Fig. 1 (top) is also applicable to the laser wakefield accelerator (LWFA) which employs a single ultrashort ($\tau_L \approx 2\omega_p^{-1}$) laser pulse. Broad bandwidth of the pulse implies that it contains a continuum of frequency pairs differing from each other by ω_p . Because the pulse is short, wake excita-

tion is not resonant, and even larger than in PBWA intensity is needed (typically, close to 10^{18} W/cm² to achieve $E/E_{WB} \sim 0.2$).

In a colliding-beam accelerator (CBA)^{15,16} we take a very different approach by employing two counter-propagating laser beams with differing frequencies: one short and another long (referred to as the pump, with duration $\tau_p = 2L_p/c$, where L_p is the length of the plasma). Two types of short laser beams are envisioned: (a) containing two spatially and temporally overlapping discrete frequency components of duration $\tau_L \gg \omega_p^{-1}$, or (b) single-frequency ultrashort ($\omega_p \tau_L \sim 1$) laser pulse. When the two beams interact in the plasma, the photons of the higher-frequency beam scatter into the photons of the lower-frequency beam. The crucial difference from the PBWA case is that now approximately twice the total photon momentum is deposited into the plasma: the recoil momentum of scattering a forward moving photon with frequency ω_0 into a backward moving photon with frequency ω_2 is $\hbar\omega_0/c - (-\hbar\omega_2/c) \approx 2\hbar\omega_0/c$. Thus, the laser beams' intensities required to produce a given accelerating field can be smaller for counter-propagating geometry than for the LWFA (or PBWA).

The bottom drawing in Fig. 1 (labeled CBA) illustrates the nonlinear excitation of the fast plasma waves which is significantly more complex than in PBWA (or LWFA). Specifically, we assume that two frequency components, separated by ω_p , are propagating in the forward direction. These two frequency components could either belong to two separate and long laser beams (as in PBWA), or to a single ultrashort laser pulse (as in LWFA). In the latter case, a continuum of such frequency pairs separated by ω_p can be identified. Only one such pair is shown in Fig. 1. The frequency phasor for the counter-propagating beam is labeled as backward beam. The beating between the different frequency components of the forward beam and the backward beam produce two "slow" plasma waves which are shown as almost-horizontal lines in the drawing. It is the nonlinear mixing of these two slow waves that gives rise to the "fast" plasma wave (labeled as plasma wake). Therefore, the accelerating plasma wave is produced by a super-beatwave: the beatwave of two beatwaves.

Visually, one can deduce from the drawing that the phase velocity of the fast wave is much larger than that of the slow waves. Mathematically, one can show that the phase velocities of the slow waves roughly scale as $v_{sl} \approx \omega_p / k_0$ while the phase velocity of the fast wake is close to the speed of light. In Sec. III we derive formulas for the fast wake amplitude and demonstrate that, under some circumstances, it can be much larger than the regular wake produced by only the forward propagating pulse(s).

III. COLLIDING BEAM ACCELERATOR

To provide motivation for the rest of the paper, we present a numerical simulation which demonstrates that the addition of a backward-propagating laser beam to a forward-propagating beam can excite very large ($\gg 1$ GeV/m) plasma waves which are stronger than the ones excited by the forward-propagating beam alone. The following physical

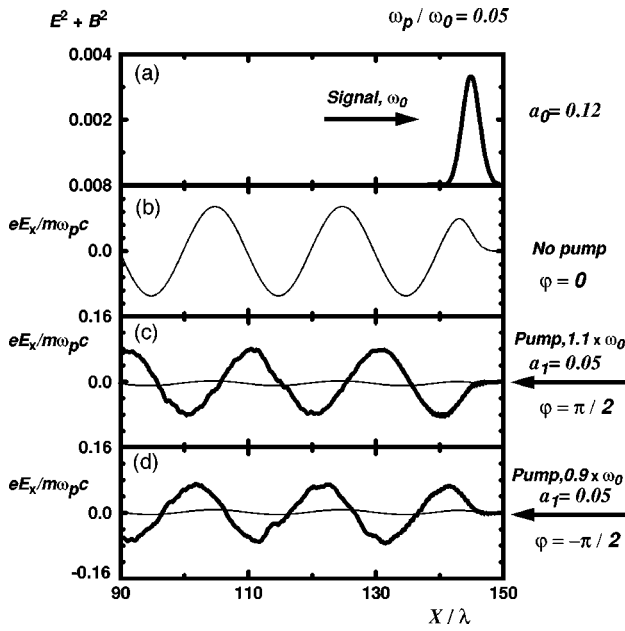


FIG. 2. Top to bottom: (a) single short laser pulse with $a_0=0.12$ and frequency ω_0 propagates from left to right; (b) short pulse generates a weak plasma wake E_x ; (c) in the presence of counter-propagating pump with $a_1=0.05$ and frequency $\omega_1=1.1\omega_0$ the wake is enhanced, and its phase is shifted by $\pi/2$ with respect to the “regular” wake of (b), which is also shown for comparison; (d) same as (c), only a down-shifted pump with $\omega_1=0.9\omega_0$ is used, and the phase shift is $-\pi/2$.

problem was simulated using a one-dimensional particle-in-cell (PIC) code VLPL.¹⁷ An ultrashort circularly polarized Gaussian laser pulse with duration $\tau_L=1.5\omega_p^{-1}$ and normalized vector potential $a_0=0.12$, propagating in the positive z direction, collides in a plasma with a long counter-propagating pulse with $a_1=0.05$. Plasma density was chosen such that $\omega_p/\omega_0=0.05$. The snapshot of the pulse intensity normalized to 2.7×10^{18} W/cm² is shown in Fig. 2(a). Two cases, corresponding to the different frequencies of the long pulse, $\omega_1=1.1\omega_0$ and $\omega_1=0.9\omega_0$, were simulated. The resulting plasma wakes are shown in Figs. 2(c) and 2(d), respectively. For comparison, we also plot the wake produced by a single short pulse *in absence* of the long counter-propagating pulse in Fig. 2(b).

Since the intensity of the short pulse is chosen nonrelativistic, the magnitude of the plasma wake left behind the pulse is much smaller than the limiting (wavebreaking) field according to $E/E_{wb}\sim a_0^2/2$, where $E_{wb}=mc\omega_p/e$. The situation changes dramatically when a counter-propagating beam is added. As Figs. 2(c) and 2(d) indicate, the addition of the pumping beam increases the electric field of the plasma wake by an order of magnitude. To further illustrate this point, we plotted the regular wake [same as shown in Fig. 2(b)] in Figs. 2(c) and 2(d) for comparison. Note that the vertical scales of the Figs. 2(c) and 2(d) and Fig. 2(b) differ by a factor 20. Plasma wakes produced as a result of the collision between the counter-propagating beams is referred to as the enhanced wake because it is much larger than the regular wake.

This conclusion about the relative magnitudes of the regular and enhanced wakes is only valid for nonrelativistic

laser pulses. It turns out that the magnitude of the enhanced wake $E < (\omega_p/\omega_0)E_{wb}$. This limit is set by the maximum velocity of the plasma electrons which cannot significantly exceed the phase velocity of the beatwave between the short and long laser beam, equal to $v_{sl}=(\omega_0-\omega_1)/2k_0$. Excitation of the fast (accelerating) plasma wake is a strongly nonlinear process, with the slow (short-wavelength) plasma waves generated as intermediaries. These short-wavelength plasma excitations can be excited either linearly, or (as it is the case for the simulation parameters of Fig. 2) nonlinearly. Below, we separately analyze these two excitation regimes, starting with the linear regime.

A. Linear regime: Four-wave mixing

The above kinematic illustration in Fig. 1 is, of course, only a cartoon, which does not explain the physical mechanism of the nonlinear mixing between the slow plasma waves. To derive the equations for the excitation of the accelerating plasma wake, assume that two laser pulses with frequencies detuned from each other by ω_p are interacting with the counter-propagating pump. Slow plasma waves are nonresonantly driven through the two-wave mixing of each of the forward-moving components of the beatwave with the pump. The beating between these slow plasma excitation is a novel mechanism of driving fast plasma waves. From Eq. (1)

$$\left(\frac{\partial^2}{\partial \zeta^2} + \omega_p^2\right)E_z = -4\pi e \frac{\partial \langle nv \rangle}{\partial \zeta}, \quad (2)$$

where $\zeta=t-z/c$, and $\langle nv \rangle = \hat{n}_0 \hat{v}_1^* + \hat{n}_1 \hat{v}_0^* + \text{c.c.}$, where $\hat{n}_{0,1}$ and $\hat{v}_{0,1}$ are, correspondingly, fractional density and velocity perturbations in the first and second slow plasma waves. The fast wave, characterized by its amplitude E_z , is then nonlinearly driven by the right-hand side (RHS) of Eq. (2). Equation (2) mathematically expresses the nonlinear mixing between the slow plasma waves schematically shown in Fig. 1.

Let us further assume that pulses 0 and 1 are both flat-tops of duration τ_L , and their corresponding detunings from the counter-propagating pump are $\Delta_0=\omega_0-\omega_2$ and $\Delta_1=\omega_1-\omega_2$. The normalized vector-potentials $a=eA/mc^2$ of the lasers are given by

$$a_{0,1} = \frac{F(t-z/v_g)}{2} a_{0,1} e^{i\theta_{0,1}} + \text{c.c.},$$

$$a_2 = \frac{a_2}{2} e_- e^{i\theta_2} + \text{c.c.}, \quad (3)$$

where $F(t)=H(t)-H(t-\tau_L)$ is the flat-top profile of the forward propagating laser beams, $\theta_{0,1}=k_{0,1}z-\omega_{0,1}t$ are their phases, and $\theta_2=k_2z+\omega_2t$ is the phase of the pumping beam which is assumed infinitely long.

Slow plasma waves are excited according to

$$\left(\frac{\partial^2}{\partial t^2} + \omega_p^2\right)\frac{\hat{n}}{n} = c^2 \nabla^2 \frac{|a|^2}{2}. \quad (4)$$

Expressing the density perturbation \hat{n} as a sum of the two slow waves

$$\hat{n} = \hat{n}_0 e^{i(k_0+k_2)z - (\omega_0-\omega_2)t} + \hat{n}_1 e^{i(k_1+k_2)z - (\omega_1-\omega_2)t} + \text{c.c.}, \quad (5)$$

we insert this expansion into Eq. (4) to obtain

$$\frac{\hat{n}_0}{n} = \frac{(k_0 + k_2)^2 c^2 a_0 a_2}{2(\Delta_0^2 - \omega_p^2)},$$

$$\frac{\hat{n}_1}{n} = \frac{(k_1 + k_2)^2 c^2 a_1 a_2}{2(\Delta_1^2 - \omega_p^2)}. \quad (6)$$

Expanding the velocity perturbations in the slow waves in the same way as it was done in Eq. (5), we calculate \hat{v}_0 and \hat{v}_1 from the continuity equation

$$\hat{v}_0 = \frac{\Delta_0}{k_0 + k_2} \frac{\hat{n}_0}{n}, \quad \hat{v}_1 = \frac{\Delta_1}{k_1 + k_2} \frac{\hat{n}_1}{n}. \quad (7)$$

We are now in a position of calculating $\langle nv \rangle$

$$\frac{\langle nv \rangle}{nc} = a_0 a_1^* \frac{F^2(t - z/v_g)}{2} e^{i(\theta_0 - \theta_1)}$$

$$\times \left[\left(\frac{\Delta_0}{k_0 + k_2} + \frac{\Delta_1}{k_1 + k_2} \right) \right]$$

$$\times \frac{(k_0 + k_2)^2 (k_1 + k_2)^2 c^3 |a_2|^2}{2(\Delta_0^2 - \omega_p^2)(\Delta_1^2 - \omega_p^2)} + \text{c.c.} \quad (8)$$

Note that the expression in front of the square brackets is proportional to the direct beatwave strength in the plasma beatwave accelerator. The term in the square brackets (which we label η) is proportional to the super-beatwave strength. Whenever the term in the square brackets exceeds unity, the super-beatwave results in a larger accelerating wake than the usual beatwave. A more compact simplified expression for η can be obtained by noting that in a tenuous plasma with $\omega_p \ll \omega_2$, $k_0, k_1 \approx k_2 \approx \omega_2/c$, yielding

$$\eta \approx 8|a_2|^2 \frac{\omega_2^3}{\omega_p^3} \left[\frac{(\Delta_0 + \Delta_1)\omega_p^3}{(\Delta_0^2 - \omega_p^2)(\Delta_1^2 - \omega_p^2)} \right]. \quad (9)$$

The magnitude of η is, roughly, determined by the quantity $8|a_2|^2 \omega_2^3 / \omega_p^3$. Equation (9) is only valid when $\Delta_{0,1}^2 \neq \omega_p^2$, which physically means that none of the slow waves are resonantly excited.

Substituting $\langle nv \rangle$ into Eq. (2), we calculate the electric field behind the forward-moving beatwave in the region $t - z/v_g > \tau_L$

$$\frac{eE_z}{mc\omega_p} = \frac{\omega_p \tau_L a_0 a_1}{4} \eta \cos(\theta_0 - \theta_1)$$

$$\approx 2|a_0 a_1 a_2|^2 \frac{\omega_2^3 \tau_L}{\omega_p^2} \left[\frac{(\Delta_0 + \Delta_1)\omega_p^3}{(\Delta_0^2 - \omega_p^2)(\Delta_1^2 - \omega_p^2)} \right]$$

$$\times \cos(\theta_0 - \theta_1), \quad (10)$$

where $\theta_0 - \theta_1 = (k_0 - k_1)z - \omega_p t$ is the phase of the fast plasma wave. Note that the phase velocity of the fast plasma wave (which is produced by the super-beatwave) is the same as that of the regular beatwave, and equal to the group velocity of the forward-moving laser packet. The phase of the fast plasma wake is determined by the relative phases of the forward-moving laser pulses. The phase of the counter-propagating pump does not matter at all, while its amplitude affects the enhancement coefficient of the super-beatwave η , thereby determining the amplitude of the fast wave as well.

Also, according to Eq. (10), fast wave generation in the colliding beam accelerator is a four-wave process.

Note that in the particular case of $\Delta_0 + \Delta_1 = 0$ wakefield vanishes. Since $\omega_1 = \omega_0 - \omega_p$, this case corresponds to $\omega_2 = \omega_0 - 0.5\omega_p$. Therefore, the scattering of the photons from beam 0 into beam 2 proceeds at the same rate as the scattering of the beam 2 into beam 1, and the overall momentum deposition into the plasma vanishes.

We simulated the beatwave enhancement using a one-dimensional particle-in-cell (PIC) code VLPL.¹⁷ Forward moving waves have identical normalized vector potentials $a_0 = a_1 = 0.025$, the counter-propagating beam has $a_2 = 0.03$. Laser and plasma frequencies were chosen as follows: $\omega_0 = 10.5\omega_p$, $\omega_1 = 9.5\omega_p$, $\omega_2 = 11.0\omega_p$. Plasma density was chosen $n = 10^{19} \text{ cm}^{-3}$ (corresponding to plasma wavelength $\lambda_p = 2\pi c/\omega_p = 10 \mu\text{m}$), beatwave pulse duration $\omega_p \tau_L = 25$, and the total simulated plasma region $L = 10\lambda_p = 100 \mu\text{m}$ long. Electric field produced as the result of the interaction is plotted in Fig. 3. The smaller signal (about 2 GeV/m) is the electric field obtained in the simulation with identical parameters, except that the pump was turned off. As Fig. 3 clearly indicates, the enhanced beatwave significantly exceeds the regular beatwave, and produces the accelerating field $E_z \approx 12 \text{ GeV/m}$.

Electric field driven by the super-beatwave appear less regular than the one driven by the regular beatwave mainly because of the finite short-wavelength electric field which is proportional to the amplitude of the slow waves. As far as the accelerating properties of the enhanced wake are concerned, short-wavelength excitations should not affect acceleration because of their low phase velocity. More on this is said in Sec. V.

Let us now turn to another scenario, which is conceptually related to the laser-wakefield accelerator (LWFA).^{1,7-11} Here an ultrashort laser pulse replaces the forward-moving beatwave. Simulation results presented in Fig. 2 assumed a large enough laser amplitude to cause the breaking of the slow plasma waves. However, at small enough laser amplitude (precisely how small is explained in the Sec. III B), linear calculation similar to the one presented for the beatwave case becomes valid. An expression for E_z , similar to Eq. (10), was derived in Ref. 15

$$\frac{eE_z}{mc\omega_p} = \frac{\pi\Delta\omega}{8\omega_0} \left(4a_2 a_0 \frac{\omega_0^2}{\omega_p^2} \right)^2 \omega_p^2 \tau_L^2 e^{-\omega_p^2 \tau_L^2 / 4}$$

$$\times \left[e^{-(\omega_p - \Delta\omega)^2 \tau_L^2} + e^{-(\omega_p + \Delta\omega)^2 \tau_L^2} + \frac{2}{3} e^{-\Delta\omega^2 \tau_L^2} \right], \quad (11)$$

where a Gaussian laser pulse $\propto \exp(-t^2/2\tau_L^2)$ was assumed. The most efficient excitation of the accelerating wake requires $\tau_L \approx 2.0\omega_p^{-1}$ and $\Delta\omega = \pm 1.1\omega_p$. For these parameters $eE_z/mc\omega_p \approx 0.6\omega_p/\omega_0 (4a_0 a_2 \omega_0^2/\omega_p^2)^2$. The enhanced wake exceeds the regular wake from forward scattering whenever $a_2 > (\omega_p/\omega_0)^{3/2}/4$. For $n_0 = 10^{18} \text{ cm}^{-3}$ and $\lambda_0 = 1 \mu\text{m}$, the corresponding critical pump intensity for which the enhanced plasma wake exceeds the regular one is given by $I_2 \approx 2 \times 10^{14} \text{ W/cm}^2$. Note that this criterion is very simi-

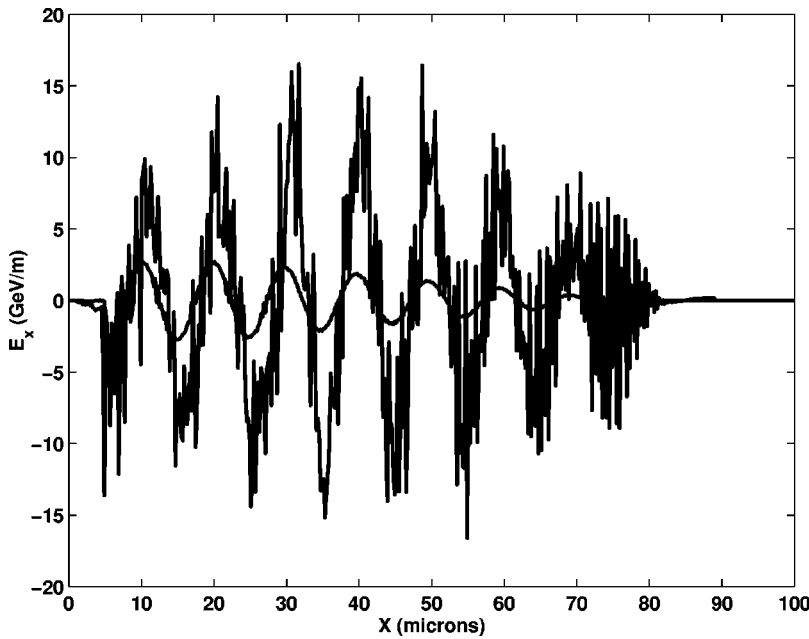


FIG. 3. Accelerating field E_z produced by the regular beatwave without pump (small wave) and with pump $a_2=0.03$ (large wave). Beatwave parameters: $\omega_0 = 10.5\omega_p$, $\omega_1 = \omega_0 - \omega_p$, $\omega_p\tau_L=25$, pump frequency: $\omega_2 = 11\omega_p$, plasma density: $n = 10^{19} \text{ cm}^{-3}$.

lar to $\eta > 1$, where η is given by Eq. (9). This is not surprising: in both cases fast plasma waves are produced via four-wave mixing.

B. Nonlinear regime: Particle trapping

The above picture of a four-wave process resulting in the excitation of a fast wave via the super-beatwave mechanism is only true when all waves in question are linear. Fast plasma wave always remains linear because its amplitude is below the wavebreaking limit. Slow waves (which beat against each other to produce the super-beatwave) break much easier, their breaking limiting the fast wave amplitude. The ease with which the slow waves break is related to their low phase velocity. Indeed, breaking of a particular wave with phase velocity v_{ph} occurs when plasma electrons are accelerated to velocities $v = v_{ph}$. After wavebreaking, particle motion is determined solely by the ponderomotive beatwave force between counter-propagating beams. Space charge force becomes smaller than the ponderomotive force, and can be neglected.

The most interesting and easy-to-understand regime corresponds to the single-frequency short pulse of duration $\tau_L < \pi/\omega_p$ which is strong enough to cause wavebreaking. The incidence of wavebreaking is, approximately, determined by the ratio of the bounce frequency $\omega_B = 2\omega_0\sqrt{a_0a_2}$ and the plasma frequency. In the strongly nonlinear regime $\omega_B^2 \gg \omega_p^2$, and the space-charge force which is proportional to ω_p^2 can be neglected in comparison with the ponderomotive force which is proportional to ω_B^2 . In this regime plasma wave amplitude is estimated¹⁶ as

$$\frac{eE_z}{mc\omega_p} = \frac{\langle P_z \rangle}{mc} \sin \omega_p \zeta \approx \text{sign}(\Delta\omega) \left(\frac{\omega_B}{\omega_0} \right) \sin \omega_p \zeta, \quad (12)$$

where $\langle P_z \rangle$ is the average momentum transferred to the plasma by the laser pulse. The physics of this momentum transfer can be visualized by plotting the electron phase

space at different times: Before the arrival of the short pulse, near the maximum of the short pulse, and right after the wavebreaking (Fig. 4).

Numerical simulations indicate that the largest momentum gain is achieved for the frequency detuning $\Delta\omega \approx \omega_B$ and pulse duration $\tau_L \approx 2/\omega_B$. For those parameters, plasma electrons execute about half a bounce in the ponderomotive potential, and leave the ponderomotive bucket with average velocity $v_z \approx c\omega_B/\omega_0$. The nonlinear current $J_{2z} = -env_z$ is then inserted into Eq. (2) to yield Eq. (12).

IV. PARAMETRIC EXCITATION OF PLASMA WAVES BY $2\omega_p$ DETUNING

In the previous section we considered two approaches to excitation of fast plasma waves: One involved two pulses moving in the forward direction and another in the backward direction (super-beatwave approach), and the other one required a short ($\tau_L \approx 2/\omega_p$) forward-moving pulse and a backward-moving pulse (CBA approach). The beatwave approach is complex for two reasons: (a) Three laser pulses are needed, and (b) laser pulses have to be detuned by the plasma frequency. Most laser systems have a fairly small bandwidth (several percent). This reduces the resonant plasma density and the accelerating gradient. For example, if the fractional frequency detuning is $\Delta\omega/\omega_0 = 3\%$, then the resonant plasma density for a $1\mu\text{m}$ laser is $n_p = 10^{18} \text{ cm}^{-3}$. Since the accelerating gradient is limited by wavebreaking to only $E_z \approx (\omega_p/\omega_0)mc\omega_p/e$, the accelerating gradient in of a super-beatwave accelerator in such plasma is only 3 GeV/m.

Single-pulse CBA can also be challenging with presently available lasers because it requires a very short pulse. For example, assuming $n_p = 10^{19} \text{ cm}^{-3}$ and $\tau_p = 2\omega_p^{-1}$ yields the full width, half maximum (FWHM) of only 14 fs. While such short pulse lasers do exist,¹⁸ they are not widely available and are, typically, low power.

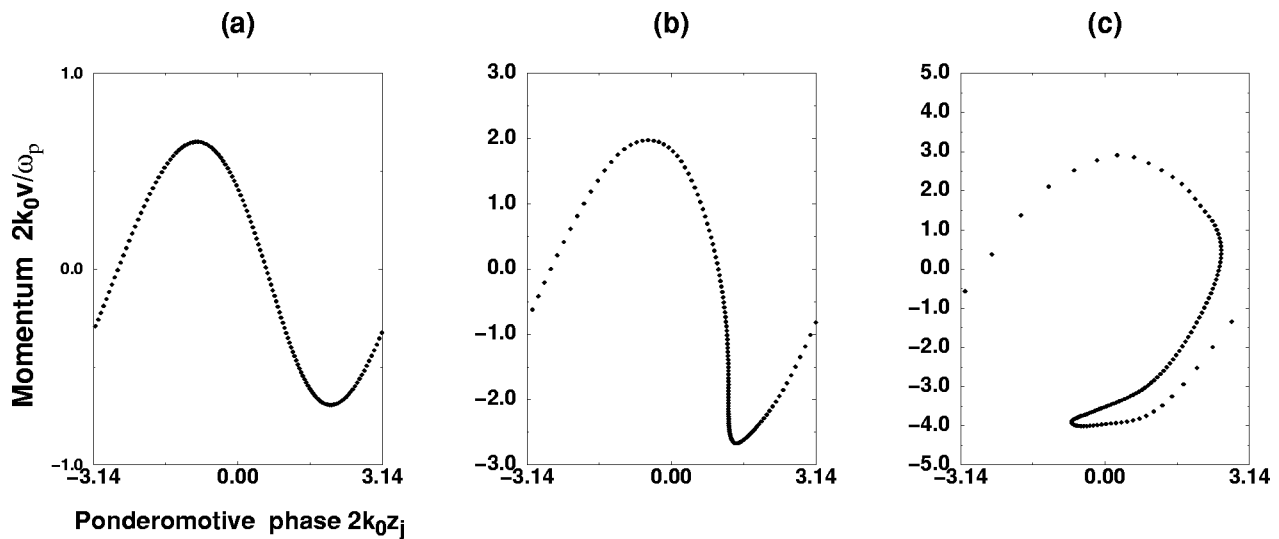


FIG. 4. Left to right: Electron phase space (a) before the arrival of short pulse; (b) near maximum of short pulse; (c) at wavebreaking. Rapid current jolt developing at wavebreaking drives the enhanced wake behind the short pulse.

All these limitations, and also the simultaneous availability of Nd:Yag ($\lambda_1 = 1.06 \mu\text{m}$) and Ti:S ($\lambda_0 = 0.8 \mu\text{m}$) laser systems in a number of laboratories compels one to think of other possible techniques of wake excitation. A novel scheme¹⁹ has been recently suggested: parametric excitation of accelerating plasma waves using counter-propagating laser beams detuned by, approximately, $2\omega_p$. Short-pulse duration no longer is required to be comparable to ω_p^{-1} ; in fact, it is advantageous to use significantly longer pulses with $\omega_p \tau_L \approx 25$. From experimental standpoint, this could be a fairly attractive regime: if $\omega_0 - \omega_1 = 2\omega_p$, then the desired plasma density $n_p \approx 2.5 \times 10^{19} \text{ cm}^{-3}$, and the required pulse duration $\tau_L \approx 25\omega_p^{-1}$ corresponds to 160 fs (FWHM). Such plasma and laser parameters are achievable, making the practical implementation of the scheme feasible.

We simulated the interaction between a trapezoidally-shaped short pulse and a long counter-propagating laser beam using a one-dimensional version of a VLPL¹⁷ particle-in-cell code. The amplitude of the circularly-polarized short pulse is $a_0 = 0.1$, its rise and fall times are $15\lambda_0/c$ and $5\lambda_0/c$, respectively, and the flat portion is $15\lambda_0/c$, where $\lambda_0 = 2\pi c/\omega_0$. The amplitude of the counter-propagating laser beam is $a_1 = 0.015$, rise and fall times are $20\lambda_0/c$, and the flat portion is $100\lambda_0/c$. Frequency of the counter-propagating beam is chosen to be $\omega_1 = 0.8\omega_0$ and the plasma frequency $\omega_p = 0.1\omega_0$.

Intensity profile of the short pulse is plotted in Fig. 5(a) 85 laser periods after it entered the plasma and interacted with the counter-propagating pumping beam. Uniform plasma extends from $Z = 5 \mu\text{m}$ to $Z = 90 \mu\text{m}$. Assuming for

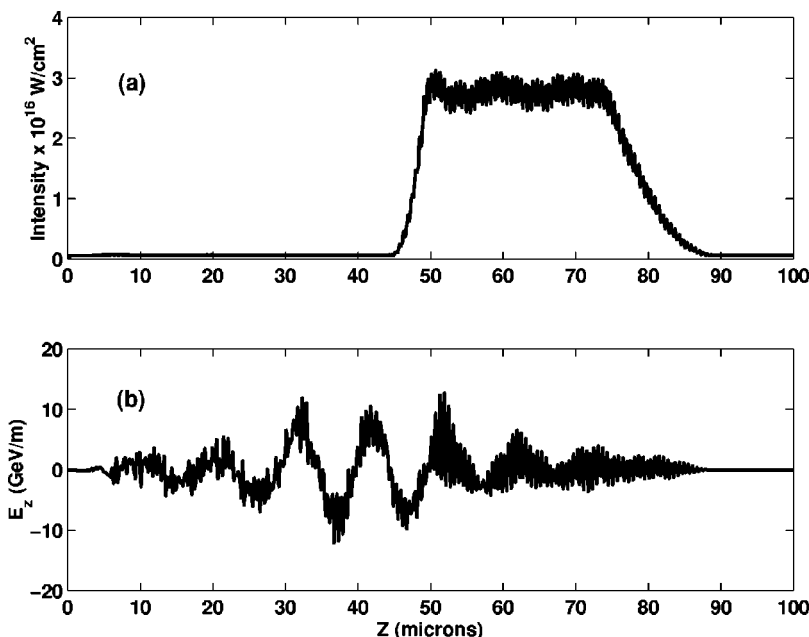


FIG. 5. Short laser pulse of trapezoidal shape ($\tau_{\text{rise}} = 15\lambda_0/c$, $\tau_{\text{drop}} = 5\lambda_0/c$, $\tau_{\text{flat}} = 15\lambda_0/c$) with amplitude $a_0 = 0.1$ and frequency ω_0 collides with counter-propagating pump with $a_1 = 0.015$ and $\omega_1 = \omega_0 - 2\omega_p$ generating an accelerating wake E_z . For $\lambda_0 = 1 \mu\text{m}$ and $\omega_p/\omega_0 = 0.1$, (a) short laser pulse intensity; (b) accelerating wakefield E_z .

simplicity that $\lambda_0 = 1 \mu\text{m}$, the peak intensity of the short pulse is $2.7 \times 10^{16} \text{ W/cm}^2$. As the short pulse interacts with the long pump, an accelerating wake grows from the front of the short pulse towards the back, as shown in Fig. 5(b). The peak accelerating gradient is about 10 GeV/m. Wakefield decreases for $Z < 20 \mu\text{m}$ because the two pulses met at $Z = 20 \mu\text{m}$.

Periodicity of the plasma wake is $10\lambda_0 = 2\pi c/\omega_p$. Therefore, the phase velocity of this wake is $\approx c$, and it is suitable for particle acceleration. The spiky appearance of the wake is due to the simultaneous generation of the slow plasma waves, just as it was the case in Fig. 3. The same simulation was repeated without the low-intensity counter-propagating beam, and the accelerating field was much smaller. This simulation confirms that the counter-propagating laser beam initiates a parametric instability which amplifies a very small initial wakefield. To our knowledge, this is the first direct PIC simulation of the plasma wake generation by two counter-propagating lasers detuned by $2\omega_p$. It confirms the effect which was previously modeled analytically and using a simplified time-averaged particle simulation.¹⁹ In the co-propagating geometry and at much higher intensity, parametric wake excitation at $\Delta\omega = 2\omega_p$ detuning was recently simulated by Ren *et al.*²⁰

That a plasma wave can be driven unstable by the $2\omega_p$ beatwave was originally proposed by Rosenbluth and Liu,¹⁴ who calculated the growth rate of a fast plasma wave $\gamma_{RL} \approx \omega_p a_0 a_1 / 2$ (co-propagating lasers). This instability is high-order, with growth rate scaling as the product of laser amplitudes. Thus, for pump waves of sub-relativistic intensity, i.e., $a_0, a_1 \ll 1$, this decay instability is too slow to be of great practical interest. Simulation results presented in Fig. 5 indicates that the *counter-propagating* geometry (i) results in a much larger growth rate, and (ii) produces fast (accelerating) plasma waves, just as the co-propagating geometry would. Both effects were overlooked in the original calculation of Rosenbluth and Liu. Thus, Fig. 5 illustrates a totally different laser-plasma instability. Below we explain the basic physics of this instability.

To describe the one-dimensional plasma motion in the field of two laser beams, we use the Lagrangian approach.²¹ Plasma electron position is characterized by its time-dependent displacement $\zeta(z_0, t)$ from the equilibrium position z_0 . By definition, $\zeta = z - z_0$ and $\zeta(z_0, t = -\infty) = 0$. Electron equation of motion is then given by

$$\ddot{\zeta}_z + \omega_p^2 \zeta_z = -\frac{e}{mc} \mathbf{v}_\perp \times \mathbf{B}_\perp \equiv -\frac{c^2}{2} \nabla |\mathbf{a}|^2, \quad (13)$$

where the second term in the left-hand side (LHS) of Eq. (13) is the restoring force of the ion background which is assumed immobile. The RHS of Eq. (13) is the ponderomotive force, and $\mathbf{a} = \mathbf{a}_0 + \mathbf{a}_1$ is the total vector potential. The expression for the ponderomotive force was derived using conservation of the canonical momenta P_x and P_y of the electron. Conservation of P_x and P_y follows from the assumption that both laser fields are given by plane waves which do not depend on x or y : $\mathbf{a}_{0,1} = a_{0,1}(\mathbf{e}_\pm \exp(i\theta_{0,1}) + \text{c.c.})$, where $\mathbf{e}_{+(-)} = (\mathbf{e}_x \pm i\mathbf{e}_y)/2$, $\theta_0 = k_0 z - \omega_0 t$, and θ_1

$= k_1 z + \omega_1 t$. In nonrelativistic case, this translates into a simple expression for $\mathbf{v}_\perp = c\mathbf{a}$ which was used to derive the equation for the ponderomotive force. We are interested in the cross-term in the expansion $|\mathbf{a}|^2 = |\mathbf{a}_0|^2 + |\mathbf{a}_1|^2 + 2\mathbf{a}_0 \cdot \mathbf{a}_1$ which is responsible for the beatwave excitation of the plasma.

Noting that $\theta_0 + \theta_1 = (k_0 + k_1)z - \Delta\omega t \approx 2k_0 z - \Delta\omega t$, where $\Delta\omega = \omega_0 - \omega_1$, we obtain from Eq. (13)

$$\ddot{\zeta} + \omega_p^2 \zeta = ik_0 c^2 a_0 a_1 e^{-2ik_0 \zeta} e^{i[\Delta\omega t - 2k_0 z_0]} + \text{c.c.} \quad (14)$$

Due to the nonlinear term $\exp(-2ik_0 \zeta)$ in the RHS of Eq. (14), several modes of plasma oscillation can become coupled. We concentrate on the coupling between two particular plasma modes with wave numbers $k_s = 2k_0 - k_p$ and $k_f = k_p \equiv \omega_p/c$. Here k_s and k_f are the wave numbers of the slow and fast plasma waves, respectively. These two waves are strongly coupled to each other when $\Delta = 2\omega_p$.

If a_0 is constant, any two waves with k_s and k_f satisfying $k_s + k_f = 2k_0$ are strongly coupled. In reality, however, a_0 represents the vector potential of an ultrashort laser pulse propagating with the group velocity $v_g \approx c$. Therefore, $a_0 \equiv a_0(t - z/v_g) \approx a_0(t - z_0/c)$ since the laser envelop is longer than the wavelength. This selects the wave number of the fast wave $k_f = \omega_p/c$ and, therefore, the wavelength of the slow wave $k_s = 2k_0 - k_p$. Numerical results presented in Fig. 5 also reveal the strong excitation of a plasma wave with $k = \omega_p/c$.

To describe the instability, we assume the most general *two-wave* ansatz for an electron displacement

$$\zeta = A_f \sin[k_p z_0 - \omega_p t + \phi_f] + A_s \sin[k_s z_0 - \omega_p t + \phi_s], \quad (15)$$

where A_f (ϕ_f) and A_s (ϕ_s) are the amplitudes (phases) of the fast and slow plasma waves. Of interest to plasma accelerators is, of course, only the fast plasma wave with phase velocity close to the speed of light. For simplicity, in the analytic calculation we assume monochromatic laser waves. Short-pulse effects are numerically treated later on (see Fig. 6).

We proceed by substituting ζ from Eq. (15) into the nonlinear term $\exp(-2ik_0 \zeta)$ in the RHS of Eq. (14) and using the Bessel identity $e^{i\alpha \sin \phi} = \sum_k J_k(\alpha) e^{ik\phi}$. Equation (14) then becomes

$$\begin{aligned} \frac{\partial^2 \zeta}{\partial t^2} + \omega_p^2 \zeta &= ik_0 c^2 a_0 a_1 \sum_{k,l} (-1)^{k+l} J_k(2k_0 A_f) J_l(2k_0 A_s) \\ &\times e^{ik[k_p z_0 - \omega_p t + \phi_f]} e^{il[k_s z_0 - \omega_p t + \phi_s]} e^{i[\Delta\omega t - 2k_0 z_0]} \\ &+ \text{c.c.}, \end{aligned} \quad (16)$$

where $\delta\omega = \Delta\omega - 2\omega_p$. A set of purely time-dependent equations can now be obtained by separating the z_0 dependent terms on both sides of Eq. (16). Thus, substituting Eq. (15) into LHS of Eq. (16) and matching the corresponding harmonics of $k_p z_0$ and $k_s z_0$ on both sides of the equation, we can write for the $(k=0, l=1)$ and $(k=1, l=0)$ terms the following:

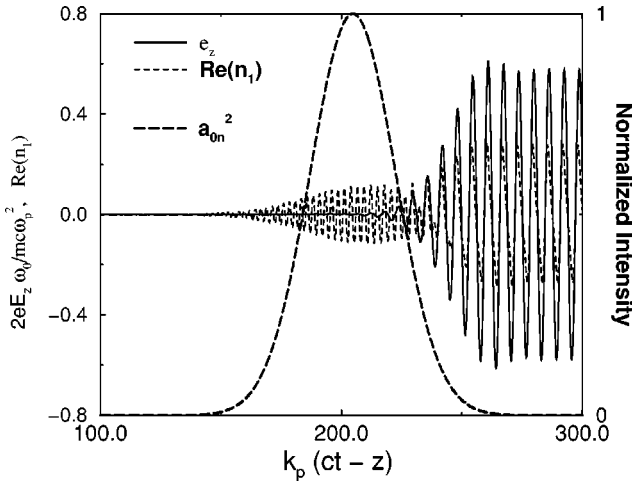


FIG. 6. Solid line: Fast electric field \bar{e}_z , long-dashed line: normalized intensity of short pulse a_0^2 , dashed line: Density bunching of the slow plasma wave $\text{Re}(\hat{n}_1) = \langle \cos \theta_j \rangle$. Rapidly varying part of \hat{n}_1 is the driven plasma response inside the laser pulse.

$$\frac{\partial \phi}{\partial t} = \delta\omega - \frac{\Omega_B^2}{4} \omega_p G(A_f, A_s) \sin \phi, \quad (17)$$

$$\frac{\partial(k_0 A_f)}{\partial(\omega_p t)} = \frac{\Omega_B^2}{4} J_0(2k_0 A_f) J_1(2k_0 A_s) \cos \phi, \quad (18)$$

$$\frac{\partial(k_0 A_s)}{\partial(\omega_p t)} = \frac{\Omega_B^2}{4} J_1(2k_0 A_f) J_0(2k_0 A_s) \cos \phi, \quad (19)$$

where $\phi = \phi_s + \phi_f + \pi/2 + \delta\omega t$, $\Omega_B^2 = 4a_0 a_1 \omega_0^2 / \omega_p^2$ is the square of the electron bounce frequency in the optical lattice created by the interference of the counter-propagating lasers, and

$$G(A_f, A_s) = \frac{J_0(2k_0 A_f) J_1(2k_0 A_s)}{k_0 A_f} + \frac{J_1(2k_0 A_f) J_0(2k_0 A_s)}{k_0 A_s}.$$

The general case of nonzero laser detuning and large wave amplitudes were analyzed in Ref. 19. Here we restrict ourselves to the resonant ($\delta\omega = 0$) and linear ($2k_0 A_{f,s} \ll 1$) case, for which Eqs. (17)–(19) are simplified to yield $\dot{\phi} = -\Omega_B^2/4(A_f/A_s + A_s/A_f) \sin \phi$, $\dot{A}_f = \Omega_B^2 A_s/4 \cos \phi$ and $\dot{A}_s = \Omega_B^2 A_f/4 \cos \phi$. Since the phase ϕ rapidly locks at $\phi = 0$, the two plasma waves, fast and slow, feed on each other and exponentiate with the growth rate $\Omega_i = \omega_0^2 a_1 a_0 / \omega_p$.

The instability mechanism is easy to understand. Fast plasma wave which varies as $\delta n_f \sim \cos \omega_p(t - z/c)$ modulates the ponderomotive force which oscillates as $f_z \sim \cos(2k_0 z - 2\omega_p t)$ to resonantly drive the slow wave which varies as $\delta n_s \sim \cos(2k_0 - k_p)z - \omega_p t$. In its turn, the slow wave modulates the ponderomotive force, driving the fast wave and completing the feedback loop of the instability. Instability persists until the wavebreaking of the slow wave. Numerical simulations indicate that the amplitude of the fast wave is limited by approximately $E_{\text{max}} = mc\omega_p^2/2\omega_0 e$.

Using a one-dimensional time-averaged particle code,²² we simulated excitation of the fast and slow plasma waves by a short slightly chirped (under-compressed) pulse with the wavelength $\lambda_0 = 0.8 \mu\text{m}$ which collides with a longer λ_1

$= 1 \mu\text{m}$ pulse in a 10^{19} cm^{-3} plasma. These wavelengths correspond to widely available laser systems (Ti:S and Nd-glass), and the plasma density was chosen to satisfy $\omega_0 = \omega_1 + 2.35\omega_p$. Other laser parameters are as follows: $a_0 = 0.15 \exp[-\zeta^2/2\tau_L^2]$ with $\tau_L = 25$ (160 fs FWHM) and $d\delta\omega/d\zeta = -9.5 \times 10^{-3} \omega_p$ (3% bandwidth). The initial fast plasma wave $\bar{e}_0 = 10^{-3}$ and $a_1 = 0.0165$ have been assumed. Simulation results are shown in Fig. 6, where we observe the excitation of both the fast and the slow plasma waves.

Despite the small amplitudes of both forward and backward pulse, and despite the fact that the duration of the short pulse is too long for the efficient wake generation, we find that a significant fast plasma wave $E_z = 7 \text{ GeV/m}$ is excited. Parameters used in the simulation are fairly standard for Ti:S and Nd-Glass systems.

Simulation results presented in Fig. 6 point to another important aspect of the parametric excitation of fast plasma waves using counter-propagating laser beams. Despite the fact that the frequency detuning between the two laser beams differs from $2\omega_p$ ($\Delta\omega = 2.35\omega_p$ in the simulation), instability still proceeds. This means that the growth rate of the instability is not very sensitive to variations in laser detuning or in the plasma density. This is quite advantageous since plasma density may not be known to high accuracy, and may vary across the interaction region.

V. UTILITY OF COLLIDING BEAM ACCELERATOR

One obvious benefit of the counter-propagating geometry is that very large accelerating wakes (of order 10 GeV/m) can be produced with moderate-intensity lasers ($I \sim 10^{16} \text{ W/cm}^2$). Another, less obvious benefit is the ability to control the phase of the accelerating wake. One observes from Fig. 2 that by changing the frequency of the long pulse from $\omega_1 = 1.1\omega_0$ [Fig. 2(c)] to $\omega_1 = 0.9\omega_0$ [Fig. 2(d)], the phase of the wake is changed by $\Delta\phi = \pi$. Thus, one can envision a “plasma linac” which consists of independently phase-controlled acceleration sections, separated by drift spaces.

Numerical implementation of the plasma linac concept is shown in Fig. 7. Collision of a short “timing beam” (TB) of duration $\tau_L = \omega_p^{-1}$ and normalized vector potential $a_0 = 0.08$ with a long “pumping beam” (PB) $a_1 = 0.012$ is modeled using a one-dimensional (1D) version of PIC simulation code VLPL.¹⁷ Figure 7(a) illustrates the temporal profile of the PB, which moves to the left; Figs. 7(b) and 7(c) are the snapshots of the generated plasma wake and the phase space of accelerated electrons, which are continuously injected with initial energy 10 MeV electrons; Fig. 7(d) shows the evolution of the TB as it moves through the plasma. To show how one can control the phase and the magnitude of the resulting plasma wake, we split the PB into two sections: The leading section of duration $\Delta t_1 = 500 \times 2\pi/\omega_0$, where $\Delta\omega = -1.7\omega_p$, and the trailing section $\Delta t_3 = 250 \times 2\pi/\omega_0$, where $\Delta\omega = 1.7\omega_p$. These two pump beam sections are separated by the middle section of duration $\Delta t_2 = \Delta t_3$, where the pump is switched off.

As Figs. 7(a) and 7(b) show, the three pump sections map into three spatial acceleration regions, which are differ-

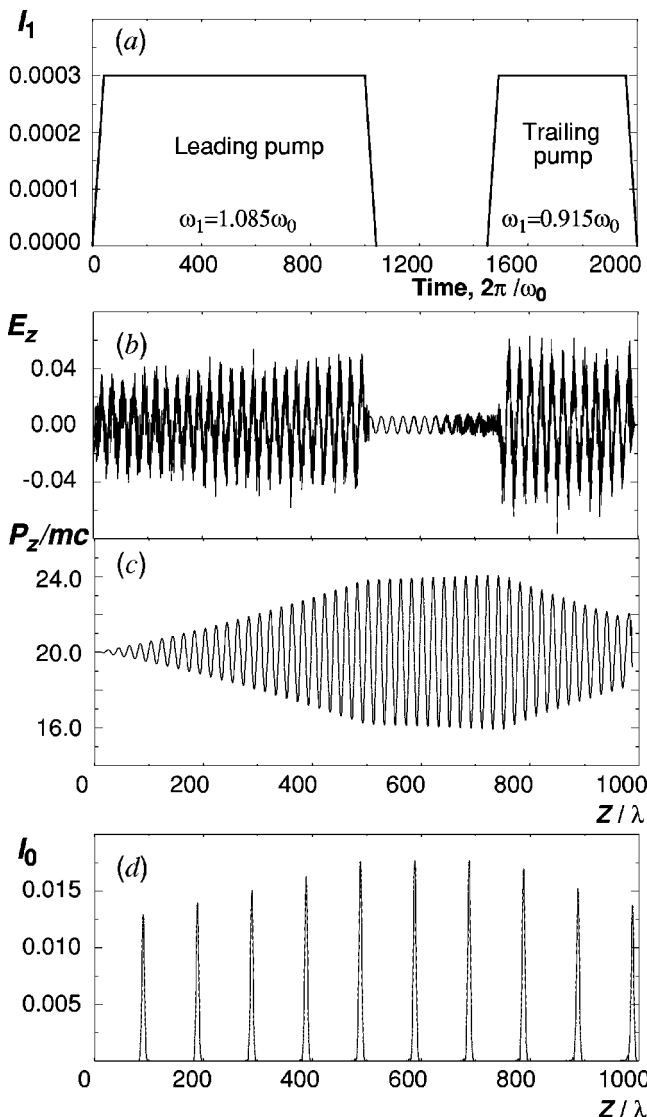


FIG. 7. Collision between a short timing beam ($a_0=0.08$, $\tau_L=\omega_p^{-1}$) and an intermittent pump ($a_1=0.012$) in $n_0=2.5\times 10^{18}$ cm $^{-3}$ plasma ($\omega_0/\omega_p=20$). 10 MeV electrons are continuously injected into the plasma. (a) Time-dependence of the pumping beam intensity $I_1=a_1^2$; (b) longitudinal electric field $eE_z/mc\omega_0$; (c) phase space of injected electrons; (d) propagation of the TB through the plasma, $I_0=a_0^2$.

ent from each other in TB dynamics, magnitude, and phase of the plasma wake. In the leading region the pump beam has higher frequency and energy flows into the TB, amplifying it. A strong plasma wake with the peak accelerating gradient of

8 GeV/m is induced. The middle region is void of the pump. Here the TB interacts with the plasma through the usual LWFA mechanism only, producing a weak, <1 GeV/m, accelerating wake. In this region the energy of the injected electrons does not significantly change, as seen from Fig. 7(c). When the trailing (low-frequency) part of the pump collides with the TB, the energy flows from the TB into the PB, Fig. 7(d). Again, a strong plasma wake is induced, Fig. 7(b). This wake, however, is shifted in phase by $\Delta\phi=\pi$ with respect to the leading region. As a result, electrons which gained energy in the leading region are decelerated in the trailing region, Fig. 7(c). This shows that both amplitude and phase of the enhanced plasma wake can be controlled by shaping the long low-intensity pump beam.

Note that the accelerating wake in Fig. 7(b) looks somewhat irregular due to the presence of the slow (short-wavelength) plasma waves. Nevertheless, the particle phase space does not show any irregularity. Relativistic particles experience a much smoother accelerating field because the phase velocity of the slow plasma waves is much smaller than the speed of light.

Plasma linac can be used to prevent phase slippage between ultrarelativistic particles and the wake which has the phase velocity $v_{ph}/c\approx 1-\omega_p^2/2\omega_0^2$. Since particles are moving slightly faster than the wake crests, they eventually outrun the accelerating phase and move into the decelerating phase of the wake (Fig. 8, left). This occurs after one dephasing length $L_d=\lambda_p^3/\lambda_0^2$. After that, acceleration has to be terminated by terminating the plasma. The next acceleration stage needs to be in phase with the previous one, presenting a serious technical challenge.

In a colliding beam plasma linac shown in Fig. 7 dephasing can be circumvented by taking the length of the leading pump section equal to $2L_d$. Particle phase dynamics is shown in Fig. 8, right. After advancing in phase by $\Delta\phi=\pi$, electron finds itself in the gap between accelerating sections. Accelerating field in the gap is very small because there is no enhanced wake there. After the gap, electron enters the second accelerating section, where the phase differs from the first section by π . Therefore, electron is in the accelerating phase again. This sequence can be repeated indefinitely, ensuring that electron is never decelerated.

VI. FUTURE WORK

An important unresolved problem is generation of accelerating plasma waves using the CBA technique in a plasma

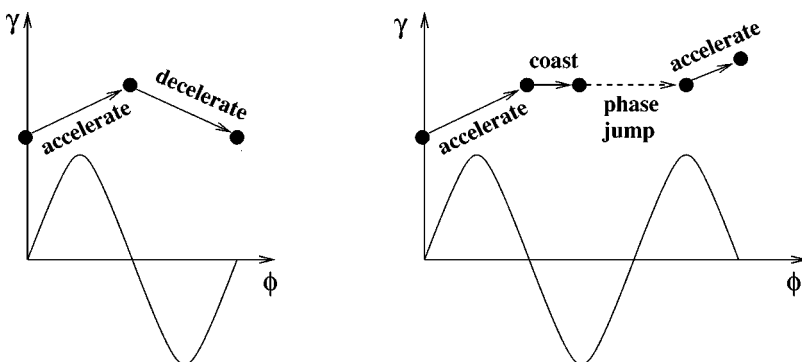


FIG. 8. Schematic of the phase slippage of electron with respect to the wake in a standard wakefield accelerator (left) and in a "plasma linac" (right).

channel. Plasma channels are important for guiding both long and short laser beams. Moreover, transversely inhomogeneous plasma may impart an unusual structure to the accelerating field with a local minimum on axis. This may result in advantageous transverse focusing properties of the wake, especially in the context of the colliding-beam injector.¹⁶

ACKNOWLEDGMENTS

This work was supported by the DOE Division of High Energy Physics and the Presidential Early Career Award for Scientists and Engineers.

¹T. Tajima and J. M. Dawson, Phys. Rev. Lett. **43**, 267 (1979).

²Y. Kitagawa, T. Matsumoto, T. Minamihata, K. Sawai, K. Matsuo, K. Mima, K. Nishihara, H. Azechi, K. A. Tanaka, H. Takabe, and S. Nakai, Phys. Rev. Lett. **68**, 48 (1992).

³C. E. Clayton, K. A. Marsh, A. Dyson, M. Everett, A. Lal, W. P. Leemans, R. Williams, and C. Joshi, Phys. Rev. Lett. **70**, 37 (1993).

⁴M. Everett, A. Lal, D. Gordon, C. E. Clayton, K. A. Marsh, and C. Joshi, Nature (London) **368**, 527 (1994).

⁵N. A. Ebrahim, J. Appl. Phys. **76**, 7645 (1994).

⁶F. Amiranoff, J. Ardonneau, M. Bercher, D. Bernard, B. Cros *et al.*, in *Advanced Accelerator Concepts*, AIP Conf. Proc. edited by P. Schoessow (American Institute Physics, New York, 1995), Vol. 335, p. 612.

⁷L. M. Gorbunov and V. I. Kirsanov, Sov. Phys. JETP **66**, 290 (1987).

⁸E. Esarey, A. Ting, P. Sprangle, and G. Joyce, Comments Plasma Phys. Controlled Fusion **12**, 191 (1989).

⁹F. Amiranoff, S. Baton, D. Bernard, B. Cross *et al.*, Phys. Rev. Lett. **81**, 995 (1998).

¹⁰K. Nakajima, T. Kawakubo, H. Nakanishi, A. Ogata *et al.*, in *Advanced Accelerator Concepts*, AIP Conf. Proc. edited by P. Schoessow (American Institute Physics, New York, 1995), Vol. 335, p. 145.

¹¹P. Sprangle, B. Hafizi, J. R. Penano, R. F. Hubbard *et al.*, Phys. Rev. E **63**, 056405 (2001).

¹²P. Chen, J. M. Dawson, R. W. Huff, and T. Katsouleas, Phys. Rev. Lett. **54**, 693 (1985).

¹³E. Esarey, P. Sprangle, J. Krall, and A. Ting, IEEE Trans. Plasma Sci. **24**, 252 (1996), and references therein.

¹⁴M. N. Rosenbluth and C. S. Liu, Phys. Rev. Lett. **29**, 701 (1972).

¹⁵G. Shvets, N. J. Fisch, A. Pukhov, and J. Meyer-ter-Vehn, Phys. Rev. E **60**, 2218 (1999).

¹⁶G. Shvets, N. J. Fisch, and A. Pukhov, IEEE Trans. Plasma Sci. **28**, 1194 (2000).

¹⁷A. Pukhov and J. Meyer-ter-Vehn, Bull. Am. Phys. Soc. **41**, 1502 (1996).

¹⁸T. Brabec and F. Krausz, Rev. Mod. Phys. **72**, 545 (2000).

¹⁹G. Shvets and N. J. Fisch, Phys. Rev. Lett. **86**, 3328 (2001).

²⁰C. Ren, E. S. Dodd, D. Gordon, and W. B. Mori, Phys. Rev. Lett. **85**, 3412 (2000).

²¹J. Dawson, Phys. Rev. **113**, 383 (1959).

²²G. Shvets, N. J. Fisch, A. Pukhov, and J. Meyer-ter-Vehn, Phys. Rev. Lett. **81**, 4879 (1998).